

THE LEVEL STRUCTURE OF ^{191}Pt FROM THE DECAY OF 3.2 h ^{191}Au

M. PIIPARINEN †, S. K. SAHA and P. J. DALY

Chemistry Department, Purdue University, W. Lafayette, Indiana 47907, USA ††

and

T. L. KHOO, C. L. DORS and F. M. BERNTHAL

*Departments of Chemistry and Physics and Cyclotron Laboratory,
 Michigan State University, East Lansing, Michigan 48824, USA †††*

Received 1 March 1976

Abstract: Levels of ^{191}Pt populated in the decay of 3.2 h ^{191}Au have been investigated by γ -ray singles and comprehensive γ - γ coincidence measurements. A detailed ^{191}Au decay scheme, which differs radically from earlier versions, has been established. The ^{191}Au decay results are discussed with reference to those obtained in complementary ($\alpha, 3n\gamma$) studies of odd- A Pt nuclei and with particular emphasis on the locations and properties of low-spin members of the $\nu i_{1/2}$ level family in ^{191}Pt .

E

RADIOACTIVITY ^{191}Au [from $^{191}\text{Ir}(\alpha, 4n)$]; measured E_γ , I_γ , $\gamma\gamma$ -coin. ^{191}Pt deduced levels, J , π , ICC. Enriched target, Ge(Li) detectors.

1. Introduction

During the course of extensive investigations of the $^{186-194}\text{Pt}$ level structures by means of (α, xn) in-beam γ -ray spectroscopy ^{1,2}), several fruitless attempts were made to discover some connections between the ^{191}Pt levels strongly populated in the $^{190}\text{Os}(\alpha, 3n)$ reaction and the low-lying ^{191}Pt levels reported in earlier radioactivity studies ³). In an effort to remedy this unsatisfactory and puzzling situation, we undertook a reinvestigation of the EC decay of 3.2 h $^{191}\text{Au}(J^\pi = \frac{3}{2}^+)$. We were hopeful that the decay study would also extend our knowledge of the $\nu i_{1/2}$ level family in ^{191}Pt by locating low-spin family members not detectably populated in the ($\alpha, 3n$) reaction.

The most notable previous study of the ^{191}Au decay was that of Johansson *et al.* ⁴), who performed comprehensive conversion electron measurements and some coincidence determinations; the ^{191}Au decay scheme presented in ref. ³) is based on their results. Surprisingly, there has been no earlier high resolution γ -ray study of the ^{191}Au decay.

† Present address: Department of Physics, University of Jyväskylä, Finland.

†† Work supported by the US ERDA.

††† Work supported by the US ERDA and the NSF.

2. Experimental procedure and data analysis

The radioactive source was produced by the $^{191}\text{Ir}(\alpha, 4n)^{191}\text{Au}$ reaction in a bombardment of 5 mg of ^{191}Ir (95 % enriched) with 50 MeV α -particles from the Michigan State University cyclotron. No chemical separation was performed since 3.2 h ^{191}Au was by far the most intense activity induced and the principal contaminant activities were those of other Au radioisotopes and of the 2.8 d ^{191}Pt decay product.

Gamma-ray singles measurements were performed using an 18 % efficiency Ge(Li) detector and a low energy photon Ge(Li) spectrometer (LEPS). The resolution of the 18 % spectrometer was 2.0 keV FWHM for 1332 keV γ -rays, and that of the LEPS was 650 eV FWHM for 122 keV γ -rays. A portion of one of the γ -ray spectra recorded with the LEPS spectrometer is shown in fig. 1. The singles measurements were started about five hours after bombardment and were continued intermittently for approximately fifteen hours. The γ -rays of ^{191}Au were identified on the basis of half-life; their energies and relative intensities are listed in table 1. The conversion electron intensities given in table 1 are those of Johansson *et al.* ⁴), normalised to the γ -ray intensities by assuming pure E2 character for the 253.95 keV transition. The electron and γ -ray intensities were combined to yield conversion coefficients and probable multiplicities for most of the transitions; these are also listed in table 1.

Extensive γ - γ coincidence measurements were performed using two Ge(Li) detectors with efficiencies of 7 % and 18 %. Three parameter (γ, γ, t) coincidence data were accumulated and stored serially on magnetic tapes. Subsequently, the prompt

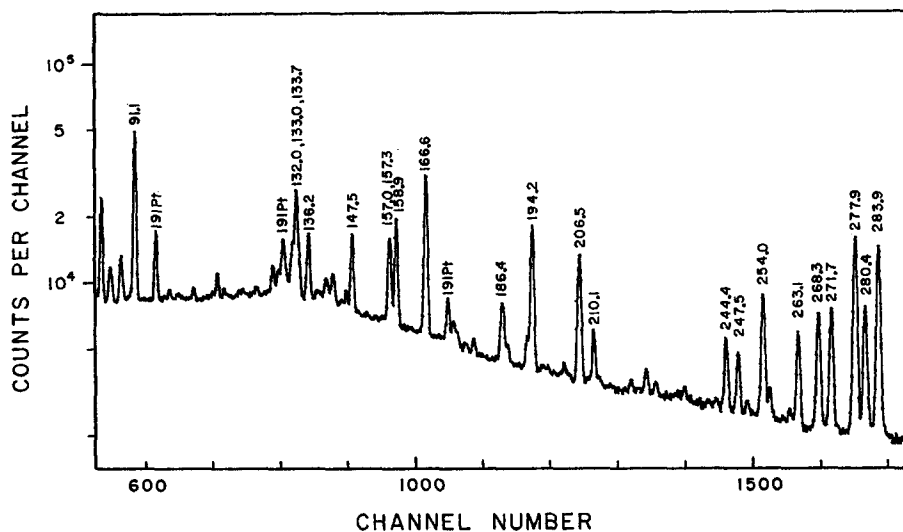


Fig. 1. A portion of the 3.2 h ^{191}Au γ -ray spectrum.

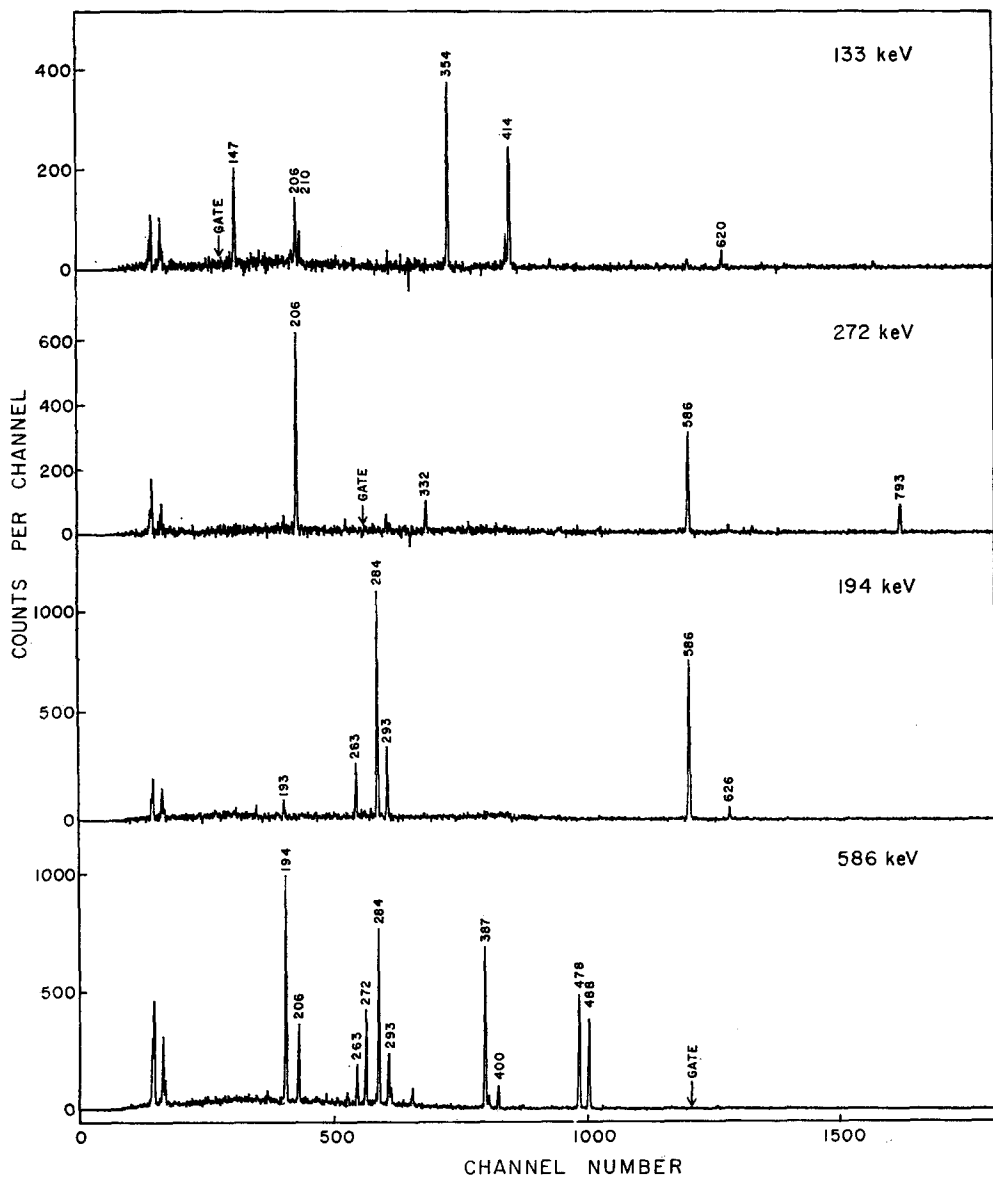


Fig. 2. Four of the γ -ray coincidence spectra recorded.

coincidence events ($2\tau \approx 50$ ns) were sorted using the MSU Sigma 7 computer, corrections for chance and Compton background coincidence events were applied, and coincidence spectra gated on about seventy different ¹⁹¹Au decay γ -rays were obtained. Some typical spectra shown in fig. 2 illustrate the high quality of the γ - γ coincidence data. These results were of prime importance in the construction of the ¹⁹¹Au decay scheme.

TABLE I
Transitions observed in ^{191}Pt following the decay of 3.2 h ^{191}Au

γ -ray energy ^{a)} (keV)	Relative γ -ray int. ^{a)}	Conversion electron int. ^{b)}	Conversion coeff. ^{b)}	Multi- polarity	Placement (keV)
24.39 ^{c)}		227(L)			173.3 \rightarrow 149.0
30.27(6)	269(40)	446(L)	1.7(L)	M1	30.3 \rightarrow 0
48.37 ^{c)}		306(L)		M2	149.0 \rightarrow 100.7
56.78(7)	19(3)				
87.55(6)	12(1)	6.2(L)	0.52(L)	M1/E2	487.6 \rightarrow 399.9
91.11(5)	99(7)	386(L)	3.9(L)	E2	100.7 \rightarrow 9.6
106.36(5)	3(1)	8	2.7	M1	399.9 \rightarrow 293.5
122.71(5)	3(1)				
126.94(5)	9(1)	15	1.7	M1/E2	293.5 \rightarrow 166.5
132.00(5)	21(2)				
132.98(4)	72(6)	144	2.0	M1	306.3 \rightarrow 173.3
133.70(5)	16(2)				
136.16(4)	40(4)	63	1.6	M1/E2	166.5 \rightarrow 30.4
142.51(5)	14(1)				
145.95(5)	6(1)	11	1.8	M1	399.9 \rightarrow 254.0
147.49(4)	51(3)	62	1.2	M1/E2	453.7 \rightarrow 306.3
156.97(5)	29(4)				166.5 \rightarrow 9.6
157.33(5)	40(6)				306.3 \rightarrow 149.0
158.89(4)	87(6)	76	0.87	M1/E2	158.9 \rightarrow 0
166.56(3)	195(14)	< 220	< 1.13	M1/E2 ^{c)}	166.5 \rightarrow 0
192.82(4)	15(2)	1.9	0.13	E2	293.5 \rightarrow 100.7
194.17(3)	161(11)	89	0.55	M1/E2	487.6 \rightarrow 293.5
202.43(4)	6(1)				
206.46(5)	130(10)	73	0.56	(M1/E2)	{660.2 \rightarrow 453.7 487.6 \rightarrow 281.2
210.09(4)	35(3)	18.5	0.53	M1/E2	1074.0 \rightarrow 863.9
223.63(5)	13(1)				254.0 \rightarrow 30.4
244.38(4)	57(4)	< 23	< 0.40	M1/E2 ^{c)}	254.0 \rightarrow 9.6
247.50(4)	44(3)	6.4	0.15	M1/E2	277.9 \rightarrow 30.4
253.95(3)	149(10)	12.4	0.083	E2	254.0 \rightarrow 0
263.09(3)	91(6)	7.5	0.082	E2	293.5 \rightarrow 30.4
268.33(4)	116(9)	30	0.26	M1/E2	277.9 \rightarrow 9.6
271.65(3)	148(10)	< 30	< 0.20	M1/E2 ^{c)}	281.2 \rightarrow 9.6
277.86(3)	424(28)	96	0.23	M1/E2	277.9 \rightarrow 0
280.40(3)	173(11)	11.2	0.065	E2	453.7 \rightarrow 173.3
283.90(3)	396(25)	74	0.19	M1/E2	293.5 \rightarrow 9.6
293.45(3)	167(11)	29	0.17	M1/E2	293.5 \rightarrow 0
316.5(5)	\approx 5				929.2 \rightarrow 613.1
332.03(5)	9(1)				613.1 \rightarrow 281.2
340.35(5)	9(1)	1.9	0.22	M1	594.3 \rightarrow 254.0
347.54(5)	32(3)				
353.88(3)	183(12)	5.7	0.031	E2	660.2 \rightarrow 306.3
359.85(5)	10(2)				613.1 \rightarrow 254.0
368.66(4)	26(2)	2.0	0.077	M1/E2	535.3 \rightarrow 166.5
376.56(4)	25(2)				535.3 \rightarrow 158.9
386.90(3)	212(14)	22.9	0.11	M1	487.6 \rightarrow 100.7
390.27(4)	160(11)	17.5	0.11	M1	399.9 \rightarrow 9.6

TABLE 1 (continued)

γ -ray energy ^{a)} (keV)	Relative γ -ray int. ^{a)}	Conversion electron int. ^{b)}	Conversion coeff. ^{b)}	Multi- polarity	Placement (keV)
399.84(4)	279(19)	7.6	0.027	E2	399.9 \rightarrow 0
408.21(6)	54(7)	3.8	0.070	M1/E2	574.7 \rightarrow 166.5
410.2(2)	26(5)	1.56	0.060	M1/E2	863.9 \rightarrow 453.7
411.5(2)	15(3)				1074.0 \rightarrow 662.3
413.73(5)	217(14)	18.5	0.085	M1/E2	1074.0 \rightarrow 660.2
421.44(4)	203(14)	15.6	0.077	M1/E2	451.8 \rightarrow 30.4
427.33(6)	13(1)	0.91	0.070	M1/E2	
432.42(10)	9(1)				
442.27(5)	35(3)	3.3	0.095	M1	451.8 \rightarrow 9.6
446.58(6)	21(2)	1.65	0.079	M1	613.1 \rightarrow 166.5
450.69(11)	9(2)				
451.85(5)	79(6)	< 5.6	< 0.071	(M1)	{ 451.8 \rightarrow 0 1113.5 \rightarrow 660.2
460.94(12)	14(2)				1074.0 \rightarrow 613.1
467.04(8)	44(6)	3.3	0.076	M1	625.9 \rightarrow 158.9
478.04(4)	232(16)	< 20	< 0.086	M1/E2 ^{c)}	487.6 \rightarrow 9.6
487.61(4)	163(11)	3.13	0.019	E2	487.6 \rightarrow 0
495.74(5)	34(3)	2.6	0.076	M1	662.3 \rightarrow 166.5
499.62(5)	27(3)				1074.0 \rightarrow 574.7
525.79(5)	51(4)	3.3	0.065	M1	535.3 \rightarrow 9.6
532.63(6)	23(3)				986.4 \rightarrow 453.7
535.25(12)	8(2)	0.37	0.044	M1/E2	
538.7(3)	48(8)	0.23	0.0049	E1	1074.0 \rightarrow 535.3
544.35(10)	9(2)				574.7 \rightarrow 30.4
557.51(8)	13(2)	0.13	0.010	E2	863.9 \rightarrow 306.3
561.59(14)	4(1)	0.31	0.08	M1	1174.4 \rightarrow 613.1
565.13(5)	29(3)	0.79	0.027	E2	574.7 \rightarrow 9.6
568.27(10)	10(2)	0.29	0.029	E2	
574.54(7)	10(2)				574.7 \rightarrow 0
580.5(3)	\approx 5				1174.4 \rightarrow 594.3
586.44(4)	1000	5.0	0.0050	E1	1074.0 \rightarrow 487.6
595.90(10)	20(2)	0.64	0.032	M1	
616.26(10)	22(3)	0.33	0.015	E2	
620.31(8)	64(6)	1.5	0.023	M1/E2	1074.0 \rightarrow 453.7
625.85(12)	53(8)	0.91	0.017	M1/E2	1113.5 \rightarrow 487.6
627.74(15)	12(3)	0.65	0.054	M1	1290.0 \rightarrow 662.3
647.97(15)	6(2)				929.2 \rightarrow 281.2
659.69(12)	17(2)	0.30	0.018	M1/E2	1113.5 \rightarrow 453.7
669.59(15)	4(1)	0.15	0.04	M1	
674.22(6)	402(29)	1.61	0.0040	E1	1074.0 \rightarrow 399.9
680.74(15)	4(1)	< 0.22	< 0.06		
701.96(12)	32(3)	0.93	0.029	M1	732.4 \rightarrow 30.4
732.48(16)	6(1)	0.13	0.02	M1	732.4 \rightarrow 0
734.51(16)	8(1)	< 0.30	< 0.04		
767.75(16)	12(2)				1074.0 \rightarrow 306.3
780.51(16)	15(2)				1074.0 \rightarrow 293.5
792.78(15)	42(4)	0.17	0.0040	E1	1074.0 \rightarrow 281.2
820.07(18)	21(2)				1074.0 \rightarrow 254.0

TABLE 1 (continued)

γ -ray energy ^{a)} (keV)	Relative γ -ray int. ^{a)}	Conversion electron int. ^{b)}	Conversion coeff. ^{b)}	Multipolarity	Placement (keV)
829.88(20)	4(1)				
835.53(16)	40(2)	0.13	0.0033	E1	1113.5 \rightarrow 277.9
854.28(20)	4(1)				
859.57(19)	18(2)				1113.5 \rightarrow 254.0
870.54(22)	6(1)	0.093	0.016	M1	
880.77(21)	11(1)				1174.4 \rightarrow 293.5
896.58(23)	8(1)				1174.4 \rightarrow 277.9
920.66(25)	5(1)	0.062	0.012	M1	1174.4 \rightarrow 254.0
1006.3(3)	4(1)				
1023.0(3)	6(1)	0.099	0.016	M1	1300.9 \rightarrow 277.9
1028.0(3)	7(1)				
1035.8(3)	5(1)	< 0.1	< 0.02		1290.0 \rightarrow 254.0
1064.7(3)	9(1)				1074.0 \rightarrow 9.6
1074.2(3)	10(1)				1074.0 \rightarrow 0
1086.9(4)	4(1)				
1096.8(3)	7(1)				
1101.9(3)	8(1)	0.103	0.013	M1	
1113.6(3)	15(2)				1113.5 \rightarrow 0
1161.2(3)	11(2)				
1164.9(3)	12(2)				1174.4 \rightarrow 9.6
1174.0(4)	8(1)				(1174.4 \rightarrow 0)
1199.3(3)	9(1)				1453.3 \rightarrow 254.0
1259.6(3)	17(2)				
1302.3(4)	9(2)				

^{a)} Uncertainties in the least significant figures are indicated in parentheses.

^{b)} K-electron intensities ⁴⁾ and K-conversion coefficients are given except where otherwise noted.

^{c)} Adopted from ref. ⁴⁾.

3. The ^{191}Au decay scheme and discussion

The ground-state spin of ^{191}Pt has recently been determined to be $\frac{3}{2}$ by the atomic beam magnetic resonance method ⁵⁾. Systematics indicate strongly that this state is derived from the $\nu p_{\frac{3}{2}}$ shell-model orbital and therefore is of negative parity. In a related in-beam study of isomerism in ^{187}Pt , ^{189}Pt and ^{191}Pt , we have determined half-lives for the $\frac{1}{2}^+$ members of the $\nu i_{\frac{3}{2}}$ families in all three nuclei ⁶⁾. The $\frac{1}{2}^+$ state in ^{191}Pt has a half-life of $95 \pm 5 \mu\text{s}$ and it de-excites by a 48.4 keV M2 transition to a $\frac{3}{2}^-$ state, which is also isomeric ($t_{\frac{1}{2}} > 1 \mu\text{s}$) and de-excites by a 91.1 keV E2 transition ⁶⁾. It is evident from table 1 that both the 48.4 and 91.1 keV transitions are observed in the ^{191}Au decay, indicating that the $^{191}\text{Pt} \frac{1}{2}^+$ isomer is populated moderately strongly following the EC decay of the $^{191}\text{Au} J^{\pi} = \frac{3}{2}^+$ ground state.

The decay scheme shown in fig. 3 was constructed on the basis of the γ - γ coincidence data, the transition intensities and multiplicities, and precise energy-sum

relationships. The most striking feature of the coincidence results was the observation in many of the coincidence spectra of triads of intense γ -rays separated by energy intervals of 9.6 and 20.8 keV. One example is the 293.5, 283.9 and 263.1 keV triad prominent in the two lowest spectra of fig. 2. In addition, several pairs of transitions differing in energy by either 9.6 or 30.4 keV were also noted (e.g. the 487.6, 478.0 keV pair in the 586 keV gate). To accommodate all these transitions, the first excited state of ¹⁹¹Pt was placed at 9.6 keV and the second excited state at 30.4 keV. This proved to be the key to the construction of the remainder of the level scheme, and it was then possible to place almost all the observed transitions in a way which was entirely consistent with the extensive coincidence data and with the transition multipolarities. Established ¹⁹¹Pt levels at 1290.0, 1300.9 and 1453.3 keV are not shown in fig. 3 because of space limitations, but the placements of the transitions de-exciting these levels are indicated in table 1.

The spin-parity of the ¹⁹¹Pt ground state is $\frac{3}{2}^-$, as noted earlier, and the present results indicate J^π values of $\frac{5}{2}^-$ and $\frac{1}{2}^-$ for the 9.6 and 30.4 keV levels, respectively. These three levels are probably analogous to the closely grouped $\frac{1}{2}^-$, $\frac{3}{2}^-$, $\frac{5}{2}^-$ levels below 14 keV excitation energy in ¹⁹³Pt [ref. 7)]. The 91.1 keV E2 transition is placed between a $\frac{9}{2}^-$ level at 100.7 keV and the 9.6 keV $\frac{5}{2}^-$ level. The 100.7 keV level is fed by 192.8 and 386.9 keV transitions as well as the 48.4 keV M2. Although coincidence relationships between the 91.1 keV γ -ray and the 192.8, 386.9 keV γ -rays were not observed because of the $> 1 \mu\text{s}$ half-life of the 100.7 keV level, the coincidence data established clearly that the 192.8 and 386.9 keV transitions de-excite the levels at 293.5 and 487.6 keV, respectively. Therefore, the placement of the 91.1 keV transition shown in fig. 3 can be considered definite, and it resolves a long-standing problem about the location of this transition in the ¹⁹¹Pt level scheme [refs. 8, 3)]. The reduced transition probability $B(E2, 91 \text{ keV})$ is less than 0.15 s.p.u., indicating that the $\frac{9}{2}^-$ level has an intrinsic configuration unlike that of the $\frac{5}{2}^-$ level at 9.6 keV. This $\frac{9}{2}^-$ configuration is probably $\nu h_{7/2}$ [ref. 6)].

The $(\alpha, 3n)$ in-beam study of ¹⁹¹Pt located a large number of high-spin positive parity levels of $\nu i_{7/2}$ character, including the $\frac{11}{2}^+$ level seen here 24.4 keV above the $\frac{13}{2}^+$ isomeric state. However, no positive parity levels with $J < \frac{11}{2}$ were detectably populated in-beam. The present ¹⁹¹Au decay study provided important missing information about the low-spin members of the $\nu i_{7/2}$ family, as is illustrated in the partial level scheme of fig. 4. The $\frac{9}{2}^+$, $\frac{7}{2}^+$ and $\frac{5}{2}^+$ levels at 306.3, 453.7 and 660.2 keV respectively [and possibly the $(\frac{3}{2}, \frac{7}{2})^+$ level at 863.9 keV] are almost certainly associated with the unique parity $\nu i_{7/2}$ orbital. The combined results from the $(\alpha, 3n)$ reaction and the ¹⁹¹Au decay study provide the most complete set of data available for an $\nu i_{7/2}$ family, and they have been used in testing the applicability to odd-*A* Pt nuclei of the model 9) of a high-*j* hole coupled to a triaxial core. For values of the asymmetry parameter γ close to 30°, this model was found to be impressively successful in accounting for the ¹⁹¹Pt data 2).

The approximate EC branching percentages and $\log ft$ values shown in fig. 3 were

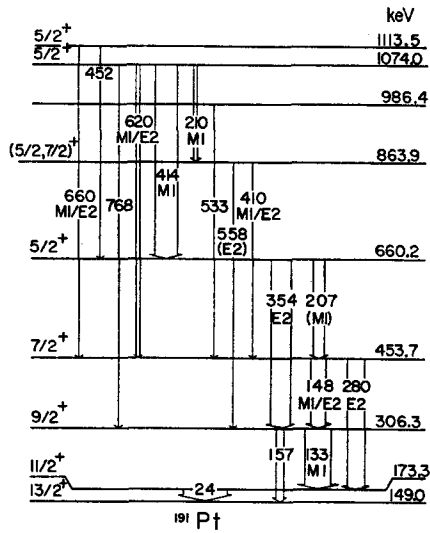


Fig. 4. A portion of the ¹⁹¹Au decay scheme showing the positive parity levels populated. Widths of transition arrows are proportional to transition intensities.

derived from intensity imbalances using an estimated decay energy $Q_{EC} = 2.0$ MeV. It was assumed that there is no EC feeding of the ¹⁹¹Pt ground state or the 9.6 keV state. Inasmuch as this is a questionable assumption, the $\log ft$ values shown should be regarded as lower limits. However it is clear that the strongest EC branch feeds the $\frac{5}{2}^+$ level at 1074.0 keV.

There is a strong resemblance between the ¹⁹¹Au decay scheme and the scheme recently reported¹⁰⁾ for the decay of 28.7 min ¹⁸⁹Au. The most intense EC branch in the ¹⁸⁹Au decay populates, with a $\log ft$ of 5.4, a positive parity level in ¹⁸⁹Pt at 1161 keV. This level and the 1074 keV $\frac{5}{2}^+$ level in ¹⁹¹Pt probably have a similar nature. To account for the low $\log ft$ value, Jastrzebski *et al.*¹⁰⁾ suggested the three quasiparticle configuration $\{\frac{3}{2}[402]\pi, \frac{1}{2}[505]\pi, \frac{3}{2}[505]\nu\}$ for the ¹⁸⁹Pt 1161 keV level. This appears to be a reasonable suggestion in good accord with level systematics; however in view of the evidence for triaxial nuclear shapes in this region²⁾, the description $(\pi d_{\frac{3}{2}}, \pi h_{\frac{5}{2}}, \nu h_{\frac{3}{2}})$ may be more suitable than one involving Nilsson orbitals appropriate to prolate nuclei. Spin-parity assignments for the lower-lying levels in ¹⁸⁹Pt were not made in ref.¹⁰⁾ Since the ¹⁸⁹Pt ground-state spin is now known⁴⁾ to be $\frac{3}{2}^-$, and the decay patterns of ¹⁸⁹Au and ¹⁹¹Au are recognizably very similar, we propose J^π values of $\frac{3}{2}^-$ and $\frac{1}{2}^-$ for the ¹⁸⁹Pt levels located¹⁰⁾ at 6.3 and 45.7 keV, respectively. If this suggestion is right, the cluster of low-lying $\frac{1}{2}^-$, $\frac{3}{2}^-$ and $\frac{5}{2}^-$ levels can be traced from ¹⁹³Pt through ¹⁹¹Pt and ¹⁸⁹Pt.

4. Conclusion

Comprehensive γ -ray singles and coincidence measurements have led to a complete revision of the ¹⁹¹Au decay scheme. Several difficulties encountered in earlier

attempts³⁾ to interpret the ^{191}Pt levels have been resolved and low-spin members of the $vi_{\frac{3}{2}}$ level family in ^{191}Pt have been located and characterized.

References

- 1) M. Piiparinen, J. C. Cunnane, P. J. Daly, C. L. Dors, F. M. Bernthal and T. L. Khoo, *Phys. Rev. Lett.* **34** (1975) 1110
- 2) T. L. Khoo, F. M. Bernthal, C. L. Dors, M. Piiparinen, S. K. Saha, P. J. Daly and J. Meyer-ter-Vehn, *Phys. Lett.* **60B** (1976) 341, and to be published
- 3) M. B. Lewis, *Nucl. Data Sheets* **9** (1973) 479 and references therein
- 4) A. Johansson, B. Nyman, G. Malmsten and S.-E. Karlsson, *Nucl. Phys.* **A98** (1967) 278
- 5) H. Rubinsztein and M. Gustafsson, *Phys. Lett.* **58B** (1975) 283
- 6) M. Piiparinen *et al.*, *Phys. Rev.* (in press)
- 7) M. B. Lewis, *Nucl. Data Sheets* **8** (1972) 389
- 8) T. W. Conlon, *Nucl. Phys.* **A100** (1967) 545
- 9) J. Meyer-ter-Vehn, *Nucl. Phys.* **A249** (1975) 111, 141
- 10) J. Jastrzebski, P. Kilcher and P. Paris, *J. de Phys.* **34** (1973) 755